Comparison between Monomeric and Polymeric Surfactants. 2. Properties of Polysurfactants in Aqueous and Nonaqueous Solution

Walter Richtering,* Rolf Löffler, and Walther Burchard

Institut für Makromolekulare Chemie, Hermann-Staudinger-Haus, Albert-Ludwigs-Universität Freiburg, Stefan-Meier Strasse 31, D-7800 Freiburg, Germany

Received December 3, 1991; Revised Manuscript Received March 18, 1992

ABSTRACT: Solution properties of nonionic polymeric surfactants in methanol and water were investigated by static and dynamic light scattering and viscometry. Common polymer behavior was observed in dilute and semidilute methanol solution. In water, a strong influence of the degree of polymerization on the solution properties was found. The high molar mass sample formed aggregates of doubled molecular weight at a low concentration. These aggregates were stable against changes of concentration and behaved like flexible chains. No influence of temperature on the solution structure was observed, even close to the lower consolute boundary. The sample of lower molar mass obeyed behavior of a polymer in a poor solvent, and strong temperature effects were found. With increasing temperature the coil contracted. In semidilute solution an excess low-angle scattering and a slow mode were detected, which revealed uncommon temperature dependence. With increasing temperature the mass fraction of the large particles decreased but the diffusive motion became slower. This effect can be caused by a strong hydrodynamic coupling due to hydrophobic interaction. The influence of the chain length on the solution properties reveals the influence of topological constraints on the thermodynamic interactions in polymeric amphiphilic systems.

1. Introduction

Amphiphilic molecules consist of a hydrophilic and a hydrophobic part, the former can be ionic or nonionic. If these molecules are dissolved in water, micellar aggregates are formed above a critical micelle concentration, cmc. The size and shape of micelles are determined by the molecular structure of the surfactant, and various types are known: spherical, wormlike, or disklike aggregates.[1-3] An often-studied group of nonionic surfactants is the poly(ethylene glycol) monoalkyl ether of the general structure $C_mH_{2m+1}(OCH_2CH_2)_nOH$ (C_mE_n). Many of these surfactants have been studied in the last 20 years, and most of the phase diagrams are known.[1,4] The aqueous solutions show two interesting features uncommon for polymers dissolved in organic solvents. (i) Isotropic micellar solutions undergo phase separation on heating. (ii) At high concentrations liquid crystalline behavior is observed with several modifications. Phase separation on heating is typical for many water-soluble polymers and is characteristic of hydrophobic interactions. The hydrophobic interaction is a complex, highly cooperative process which cannot satisfactorily be described by simple interaction among hydrated segments but results from a change of order in the water structure, induced by an attractive interaction of a hydrophobic segment with water molecules.[5-7] Thus, hydrophobic interaction is a specific feature of aqueous solutions which makes investigation of surfactants and water-soluble polymers interesting.

In the case of low molar mass surfactants, like those of the C_mE_n-type, studies of the solution's structure are difficult because the size and shape of the micelles may change with temperature and concentration. Many papers are dedicated to this problem, and different models like anisotropic growth[8-10] or statistical association are discussed.[11-13]

In polymer surfactants the amphiphilic molecules are covalently connected to macromolecules. This chemical fixation strongly influences solution properties. A cmc may no longer be observed, because a macromolecule itself can act as a "micelle"; e.g., solubilization of hydrophobic molecules is already possible by one polymer, and self-assembling is not necessary. Furthermore, the polymer's shape in solution can be expected to depend on the degree of polymerization. Due to its amphiphilic structure the macromolecule will try to minimize contacts between the hydrophobic part and water. Topological constraints may arise if the degree of polymerization exceeds the aggregation number of the corresponding monomer micelle. Consequently, it might be possible to induce a certain (e.g., rodlike) shape of the polymer in solution by varying the chain length. It is also interesting whether liquid crystalline mesophases are observed. In the case of low molar mass surfactants liquid crystalline phases are probably built up by micelles;[14] in polymer systems different possibilities might be discussed. Ordering may occur between aggregates or individual chains or even subregions of macromolecules.

It seems to be obvious that polymeric surfactants will combine polymer and surfactant properties, and we were rather certain that it would be possible to separate these two influences. It should be possible to study the polymeric properties in nonaqueous solution where no hydrophobic interactions are present.

In this paper a polysurfactant was studied which was polymerized at the hydrophobic end. The monomeric unit has the following structure:

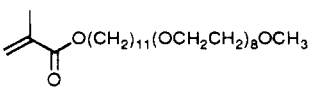

Phase behavior in water of the monomer[15] and polymer, respectively, was recorded (Figure 1). In both cases a lower consolute boundary and a hexagonal liquid crystalline phase are observed. Polymerization stabilizes the mesophase concerning the temperature and concentration range. A detailed description of the phase diagrams is given elsewhere.[16] Properties of dilute and semidilute solutions of the monomer were investigated by static and dynamic light scattering. The surfactant forms small spherical micelles with a molar mass of 44 000 g/mol and a radius of 3.4 nm. At high temperatures the small mi-

0024-9297/92/2225-3642$03.00/0

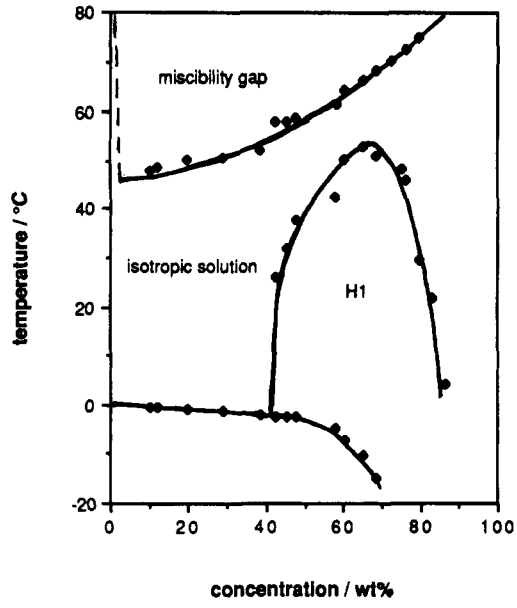

Figure 1. Phase diagram of $PMC_{11}E_8$-1 in water.

celles aggregate to random clusters. A more detailed description of the solution properties of the monomer is given in a separate paper.[15]

The present paper is organized as follows. After short experimental and theoretical sections the characterization of the polysurfactants in methanol is reported before aqueous solutions are discussed. In both cases results from dilute and semidilute solutions are presented separately. Finally some conclusions are discussed.

2. Experimental Section

The preparation of monomer and polymers is described in ref 16. Static and dynamic light scattering have been measured simultaneously with an automatic ALV goniometer and an ALV Structurator/Correlator ALV 3000. In semidilute solution time correlation functions were measured in the multiple-τ mode using 192 channels starting with a sampling time of 1 μs, plus 16 fast real channels with STC = 60 ns. An argon and a krypton ion laser were used as light sources, the wavelength being λ_0 = 496.5 and 647.1 nm, respectively. The refractive index increment was measured with a Brice Phoenix differential refractometer and was found to be (at λ_0 = 488 nm)

In methanol: $dn/dc = 0.160$

In water: $dn/dc = 0.145 - [0.0004(T - 15)]$

(dn/dc in mL/g; T in °C).

Solutions were prepared by filtration through Millipore filters. Viscosity measurements were performed with an Ubbelohde viscosimeter and a Haake Rotovisco RV 100 instrument using a couette system according to Mooney–Edward (shear rate 0–60 s^{-1}).

3. Theoretical Background

Static light scattering from dilute solutions is commonly described by the equation[17]

$$\frac{Kc}{R(\theta)} = \frac{1}{M_w}\left(1 + \frac{1}{3}\langle s^2\rangle_z q^2\right) + 2A_2c + 3A_3c^2 + \dots \quad (1)$$

with $q = (4\pi/\lambda)\sin(\theta/2)$ and the other symbols having the usual meaning. Measurements at finite angle and concentration are extrapolated in a Zimm plot and permit the characterization of the properties of a single macromolecule in solution.

At zero scattering angle the osmotic modulus $(1/RT)\cdot(\partial\pi/\partial c)$ (=inverse osmotic compressibility) is obtained.

$$\frac{Kc}{R(\theta=0)} = \frac{1}{RT}\frac{\partial\pi}{\partial c} = \frac{1}{M_{app}} \quad (2)$$

This expression is valid for all polymer concentrations. Theory shows that the reduced osmotic modulus $(M_w/RT)(\partial\pi/\partial c)$ depends on the dimensionless parameter $X = A_2M_wc$.[18,19] X is proportional to c/c^* where c^* is the overlap concentration. Relations for hard spheres (Carnahan–Starling equation[20]) and flexible chains (renormalization group theory[18]) are known and the influence of the polymer's architecture on the concentration dependence of the osmotic modulus was found experimentally.[21]

The angular dependence of the scattered light can be described for all concentrations by the common equation[22]

$$Kc/R(q) = M_{app}^{-1}(1 + \xi^2q^2) \quad (3)$$

In dilute solution the correlation length ξ corresponds to the apparent radius of gyration $\xi^2 = \langle s^2\rangle_{app}/3$ which decreases due to thermodynamic forces. The influence of thermodynamic interactions can be taken into account, and the corrected correlation length should be constant at low concentrations and decreases in semidilute solution with the formation of a homogeneous entanglement network.

In dynamic light scattering a time correlation function is measured and the first cumulant Γ is determined.[23] Extrapolation of $D_{app} = \Gamma/q^2$ to zero angle yields the mutual diffusion coefficient. In dilute solution the concentration dependence can be described by the common linear equation

$$D_c = D_z^0(1 + k_Dc) \quad (4)$$

and by use of the Stokes–Einstein law a hydrodynamic radius R_h can be calculated from D_z^0.

Irreversible thermodynamics show that the mutual diffusion coefficient depends on both thermodynamical and frictional interactions:[24]

$$D_c = (k_BT/f_c)[(M_w/RT)(\partial\pi/\partial c)] = (k_BT/f_c)[M_wKc/R_{\theta=0}] \quad (5)$$

where k_B is Boltzmann's constant and f_c is the concentration-dependent friction coefficient.

4. Solution Behavior in Methanol

Nonaqueous solutions can be chosen to separate the polymer behavior of polysurfactants from the surfactant behavior. In this study methanol was used as solvent for two reasons: (i) the low molecular weight surfactant $C_{14}E_8$ showed no formation of aggregates in methanol, and (ii) in a recent study of a similar polysurfactant $PMC_{10}E_6$ in methanol, identical results were obtained at different temperatures.[25] Both observations indicate that methanol does not give rise to association of amphiphilic molecules and therefore permits the characterization of the polymer properties.

4.1. Results. Two samples of $PMC_{11}E_8$ were available for this study. The results from light scattering experiments in dilute solution are summarized in Table I. The number-average molar mass was obtained from membrane osmometry, and a rather broad polydispersity of M_w/M_n = 2.9 was found for both samples.

The concentration dependence of the reduced osmotic modulus of the polysurfactants in methanol in *semidilute* solution is shown in Figure 2 together with the theoretical curves for hard spheres and flexible chains. Both samples

Table I
Results from Light Scattering from $PMC_{11}E_8$-1 and $PMC_{11}E_8$-2 in Methanol

	M_w, g/mol	A_2, mol·cm³·g⁻²	$\langle s^2\rangle_z^{0.5}$, nm	D_z^0, cm²/s	R_h, nm	k_D, cm³/g	ρ
$PMC_{11}E_8$-1	6.23×10^5	1.27×10^{-4}	32.3	2.13×10^{-7}	16.9	30	1.91
$PMC_{11}E_8$-2	2.87×10^5	1.04×10^{-4}	23.5	2.86×10^{-7}	12.6	15	1.87

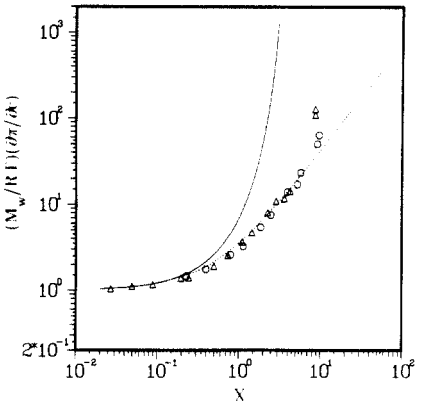

Figure 2. Plot of the reduced osmotic modulus of the polysurfactants in methanol vs the parameter $X = A_2M_wc$: $PMC_{11}E_8$-1 (○), $PMC_{11}E_8$-2 (△), hard spheres (—), flexible chains (···).

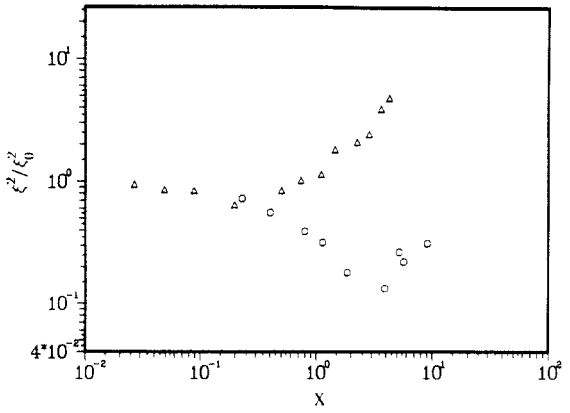

Figure 3. Plot of the square reduced correlation length of $PMC_{11}E_8$-1 (○) and $PMC_{11}E_8$-2 (△) in methanol vs the parameter X.

followed the flexible-chain behavior up to $X = 6$, and then a slightly stronger repulsion was observed with $PMC_{11}E_8$-2, i.e., the lower molar mass. In Figure 3 the square uncorrected correlation length ξ^2, normalized by the correlation length at zero concentration ξ_0^2, is plotted versus the parameter X. An increase was observed with both samples at high concentrations, indicating a formation of larger particles. A similar behavior was found in dynamic light scattering. With $PMC_{11}E_8$-2 a downturn of D_c, obtained from the first cumulant, is observed. Therefore, the time correlation function was measured over long delay times and analyzed by inverse Laplace transformation with the CONTIN program.[26] Two relaxation processes were observed, and the relaxation times differed by more than 2 orders of magnitude. Multiple-τ measurements of the time correlation function were performed at two temperatures, and the diffusion coefficients obtained from CONTIN analysis are listed in Table II.

4.2. Discussion. The molar mass of both samples exceeds that of the monomer micelle in water ($M_w = 44\,000$ g/mol).[15] The angular dependence is linear, and the ρ-parameter, which is the ratio of the radius of gyration and hydrodynamic radius,[27] reveals common linear chain behavior. The molecular weight dependence of the second virial coefficient, however, does not follow a common relationship. Usually A_2 decreases with increasing molecular weight, but here the sample with lower molar mass has a smaller A_2. This can be a consequence of a difference in the solvent quality for the hydrophilic and hydrophobic part of the molecule. Methanol is a good solvent for poly(ethylene glycol) but a poor solvent for poly(methyl methacrylate). Therefore, the free energy of the macromolecule may depend on the chain conformation in a specific manner, because unfavorable contacts can occur due to geometrical restrictions. In such a case the second virial coefficient, which describes the interaction of solvated macromolecules, will depend on the chain length in a slightly unusual manner.

Table II
Results from CONTIN Analysis of the Time Correlation Function (D in cm²/s) of $PMC_{11}E_8$-2 in Methanol

concn, g/L	$T = 20$ °C	$T = 40$ °C
96	$D_{coop} = 1.04 \times 10^{-6}$	$D_{coop} = 1.42 \times 10^{-6}$
96	$D_{slow} = 8.4 \times 10^{-9}$	$D_{slow} = 1.42 \times 10^{-8}$
143	$D_{coop} = 1.32 \times 10^{-6}$	$D_{coop} = 1.84 \times 10^{-6}$
143	$D_{slow} = 3.6 \times 10^{-9}$	$D_{slow} = 4.9 \times 10^{-9}$
290	$D_{coop} = 1.59 \times 10^{-6}$	$D_{coop} = 2.28 \times 10^{-6}$
290	$D_{slow} = 8.5 \times 10^{-10}$	$D_{slow} = 1.35 \times 10^{-9}$

Semidilute solutions also reveal interesting behavior. The concentration dependence of the osmotic modulus follows the behavior of linear flexible macromolecules. The correlation length, however, increases at high concentrations, which is not expected but indicates the formation of larger particles. Cluster formation has been observed in many different semidilute polymer solutions.[21] Often two observations have been made: (i) In static light scattering an excess low-angle scattering is found leading to an increase in M_{app} and consequently causing a turnover of the osmotic modulus to lower values. (ii) In dynamic light scattering a slow mode is detected. Due to the coincidence of both effects, it was suggested that large clusters are formed.[28] In the present case of polysurfactants, however, the increase of the correlation length is accompanied by a slow mode but not by an increase of M_{app}. The osmotic modulus does not turn over. The reason for this behavior is not yet fully understood, but a conjecture may be given. Due to the blocklike structure of the side groups some kind of local phase separation may occur between ethylene glycol and alkyl domains. Such a process would cause an increase of the correlation length and a slow diffusion. The separated domains are more compact and will show strong excluded-volume effects, similar to those of hard spheres. The repulsive forces can compensate the increase of mass in a manner such that the apparent osmotic modulus as a whole does not change strongly.

If the temperature is increased, both relaxation processes become faster. The increase of the D_{coop} is governed by the change of temperature and solvent viscosity. The slow diffusion coefficient shows a stronger increase than by a factor of T/η_0, indicating that the domains "melt" at high temperatures.

5. Behavior in Aqueous Solution

5.1. Results. Phase Diagram. The phase diagram of $PMC_{11}E_8$-1 is shown in Figure 1. A hexagonal phase (H1) was observed in the concentration range from 40 to 90% surfactant independent of molar mass. The clearing tem-

Table III
Results from Light Scattering of $PMC_{11}E_8$-1 in Water at $c > 2$ g/L

T, °C	M_w, g/mol	A_2, mol·cm³·g⁻²	$\langle s^2\rangle_z^{0.5}$, nm	D_z^0, cm²/s	R_h, nm	k_D, cm³/g	ρ
15	1.22×10^6	3.0×10^{-5}	49.4	8.7×10^{-8}	21.3	18	2.3
20	1.26×10^6	2.63×10^{-5}	42	1.03×10^{-7}	20.8	14	2.0
30	1.24×10^6	2.48×10^{-5}	40.6	1.34×10^{-7}	20.8	16	1.95
40	1.28×10^6	1.76×10^{-5}	40.7	1.84×10^{-7}	19.1	4.9	2.1

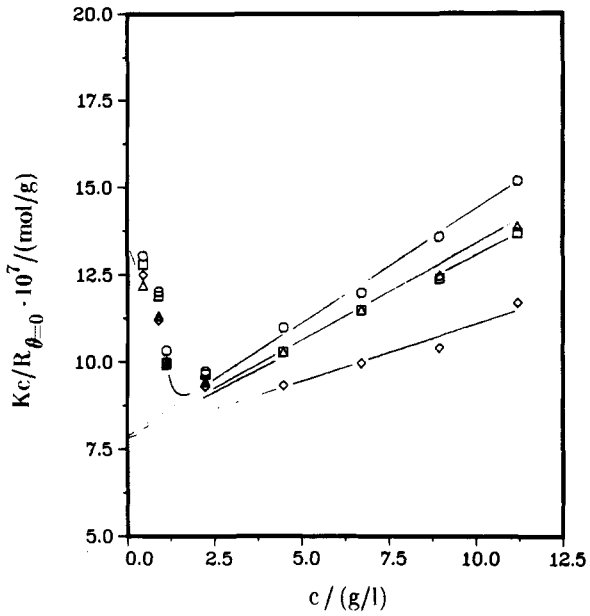

Figure 4. Concentration dependence of static light scattering at zero scattering angle from $PMC_{11}E_8$-1 in water at different temperatures: 15 °C (○), 20 °C (△), 30 °C (□), 40 °C (◇).

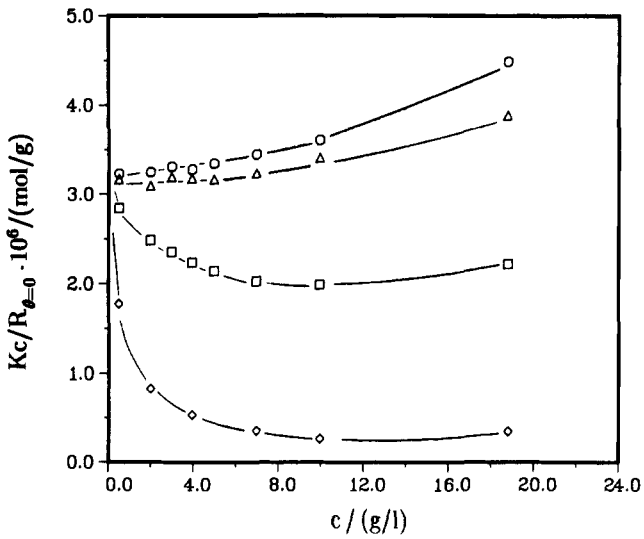

Figure 5. Concentration dependence of static light scattering at zero scattering angle from $PMC_{11}E_8$-2 in water at different temperatures: 20 °C (○), 30 °C (△), 40 °C (□), 52 °C (◇).

perature was 54 °C at about 65%. The lower critical solution temperature (LCST) depended on the degree of polymerization, LCST = 45 °C was found for $PMC_{11}E_8$-1 and LCST = 53 °C for $PMC_{11}E_8$-2. Therefore, investigations of isotropic solutions were performed in different temperature ranges for the two samples. $PMC_{11}E_8$-1 was studied between 15 and 40 °C and the second sample between 20 and 52 °C.

Dilute Solutions. The properties of aqueous solutions differ strongly from those in methanol. In Figures 4 and 5 the concentration dependence of static light scattering at different temperatures is shown. For the sake of clearness only the extrapolated values at zero scattering angle are plotted. In both cases uncommon concentration and temperature dependences were observed.

Table IV
Results from Light Scattering from $PMC_{11}E_8$-1 in Water at $c < 2$ g/L

T, °C	M_w, g/mol	$\langle s^2\rangle_z^{0.5}$, nm	D_z^0, cm²/s	R_h, nm	ρ
15	6.8×10^5	34	1.11×10^{-7}	16.7	2.0
20	7.1×10^5	35	1.23×10^{-7}	17.4	2.0
30	6.9×10^5	33	1.68×10^{-7}	16.6	2.0
40	7.3×10^5	32	2.11×10^{-7}	16.7	1.9

With the first sample, $PMC_{11}E_8$-1, a minimum at about 2 g/L was found for all temperatures. The radius of gyration exhibited a maximum and the diffusion coefficient a minimum at this concentration. Such behavior is typical of a closed association, in which molecules aggregate up to a certain concentration.[29] Evaluation of the data can now be performed in two ways. Extrapolation of measurements below $c = 2$ g/L yields information on the single macromolecule; extrapolation of measurements at $c > 2$ g/L gives details on the structure of the aggregates. The results are summarized in Tables III and IV. In both concentration regimes the results were independent of temperature. Results at $c < 2$ g/L are in good agreement with those obtained in methanol; the molar mass was slightly higher.

The lower molecular weight sample, $PMC_{11}E_8$-2, revealed a different behavior. In the Zimm diagram no minimum was observed at low temperatures. At 30 °C the second virial coefficient vanished; i.e., a θ-point was reached. At higher temperatures a minimum at about 10 g/L was found, but it was broader than that found for $PMC_{11}E_8$-1 (Figure 5). If the measurements below 10 g/L are extrapolated to zero concentration (see Table V), a temperature-independent molar mass is found which again is slightly higher than that in methanol. The dimensions, however, were smaller than those in methanol, and with increasing temperature, the radius of gyration and ρ-parameter decreased, indicating a coil contraction.

Aqueous solutions of $PMC_{11}E_8$-2 had also been investigated by viscometry. Two features of viscosity behavior had been studied, namely, the zero-shear viscosity η for different temperatures and concentrations and the intrinsic viscosity $[\eta]$ at 20 °C.

The viscosity behavior is similar to that of the monomeric system.[15] In the whole region Newtonian flow behavior is observed. At higher temperatures ($T > 30$ °C) an increase in the viscosity is found. A similar behavior was also found for the monomeric compound $MC_{11}E_8$, but the increase of the viscosity for $PMC_{11}E_8$-2 is more pronounced close to the phase-separation temperature. To exclude the influence of concentration and intermolecular hydrodynamic correlation, we have determined the intrinsic viscosity $[\eta]$ at 20 °C (see Figure 6). A surprisingly low intrinsic viscosity of 10 mL/g was determined, which corresponds to an increase of a factor of 2, compared to the monomer micelle in water.

Semidilute Solutions. In Figure 7 the reduced osmotic modulus of the aggregates of $PMC_{11}E_8$-1 is plotted vs the parameter $X = A_2M_wc$. A common curve was observed

Table V
Results from Light Scattering of $PMC_{11}E_8$-2 in Water at $c < 10$ g/L

T, °C	M_w, g/mol	A_2, mol·cm³·g⁻²	$\langle s^2\rangle_z^{0.5}$, nm	D_z^0, cm²/s	R_h, nm	k_D, cm³/g	ρ
20	3.11×10^5	1.0×10^{-5}	18.1	2.18×10^{-7}	9.8	3	1.84
30	3.15×10^5	0	17.6	2.80×10^{-7}	9.9	0	1.78
40	3.12×10^5	<0	16.4	3.73×10^{-7}	9.4	-29	1.74
45	3.12×10^5	<0	14	4.20×10^{-7}	9.3	<0	1.46
52	3.12×10^5	<0	10	4.60×10^{-7}	9.8	<0	1.05

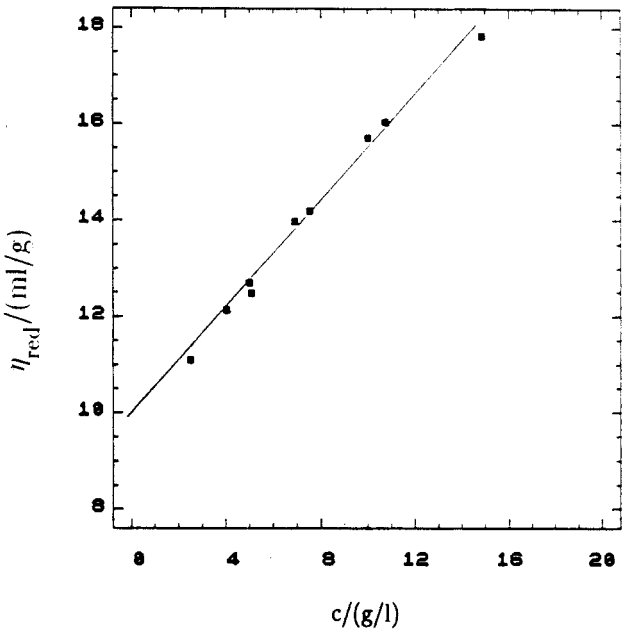

Figure 6. Concentration dependence of the reduced viscosity of $PMC_{11}E_8$-2 in water at 20 °C.

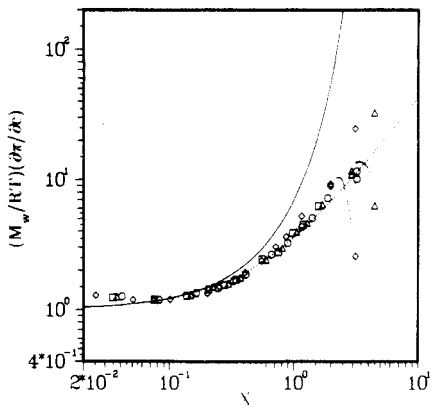

Figure 7. Plot of the reduced osmotic modulus of $PMC_{11}E_8$-1 in water at different temperatures vs $X = A_2M_wc$: 15 °C (○), 20 °C (△), 30 °C (□), 40 °C (◇).

for all temperatures, which followed flexible-chain behavior up to $X = 2$. At high concentrations a small-angle excess scattering was observed; therefore, two points are plotted in Figure 7, corresponding to the measurements at small and large angles, respectively. The former lead to a turnover of the osmotic modulus; the latter, which describe the osmotic modulus of an entanglement network, were now slightly higher than the theoretical curve. A temperature dependence was observed with the excess scattering; it decreased with increasing temperature. The corresponding plot of the diffusion coefficient is shown in Figure 8. At concentrations where the excess scattering was observed in static light scattering, the apparent diffusion coefficient decreased.

With $PMC_{11}E_8$-2 a definition of c^* via the second virial coefficient is not possible. Therefore, the osmotic modulus, radius of gyration, and diffusion coefficient are plotted directly vs concentration in Figures 9–11. At high concentrations a slope of 2.1 was observed for the osmotic modulus, independent of temperature. Again low-angle excess scattering was observed at high concentrations which vanished after the temperature was increased (see Figure 12). Simultaneously a slow mode was detected in the time correlation function of dynamic light scattering;

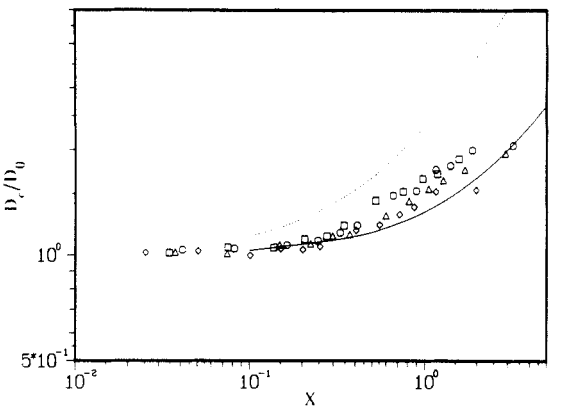

Figure 8. Plot of the reduced diffusion coefficient of $PMC_{11}E_8$-1 in water at different temperatures vs X: 15 °C (○), 20 °C (△), 30 °C (□), 40 °C (◇), hard spheres (—), flexible chains (···).

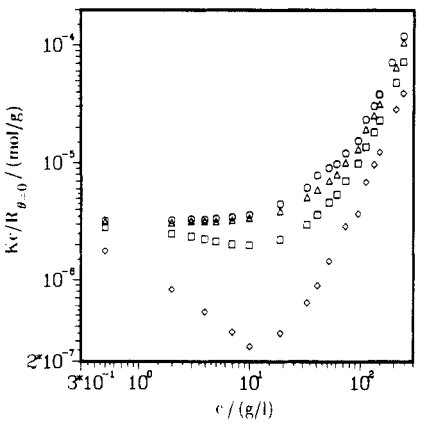

Figure 9. Concentration dependence of the osmotic modulus of $PMC_{11}E_8$-2 in water at different temperatures: 20 °C (○), 30 °C (△), 40 °C (□), 52 °C (◇).

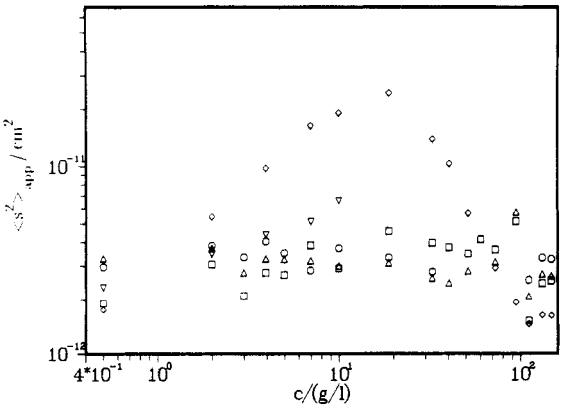

Figure 10. Concentration dependence of the square apparent radius of gyration of $PMC_{11}E_8$-2 in water at different temperatures: 20 °C (○), 30 °C (△), 40 °C (□), 45 °C (▽), 52 °C (◇).

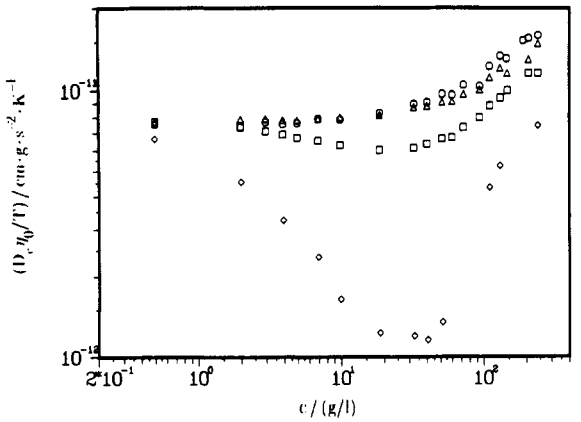

Figure 11. Concentration dependence of the diffusion coefficient, normalized by T and η_0, of $PMC_{11}E_8$-2 in water at different temperatures: 20 °C (○), 30 °C (△), 40 °C (□), 52 °C (◇).

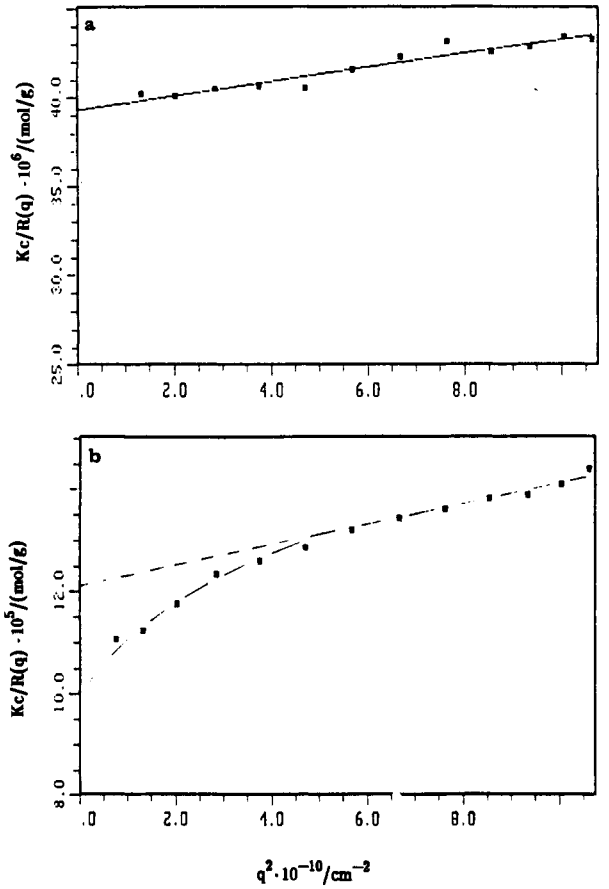

Figure 12. Angular dependence of static light scattering from a 24% solution of $PMC_{11}E_8$-2 in water at 52 (a) and 20 °C (b).

however, a surprising influence of temperature was observed. After increasing the temperature, the height of the plateau in the time correlation function decreased, corresponding to the decrease of excess scattering; the relaxation time, however, became longer (Figure 13). The results from the CONTIN analysis are summarized in Tables VI and VII.

5.2. Discussion. The molar mass of both samples was higher than the molar mass of the monomer micelle. Therefore, the polymer cannot have the same structure in solution as the monomer micelle and totally different solution properties were found. The measurements in dilute and semidilute aqueous solution revealed not only that the behavior was different from the monomer but also that the two samples behaved very differently, although the degrees of polymerization differed only by a factor of 2.

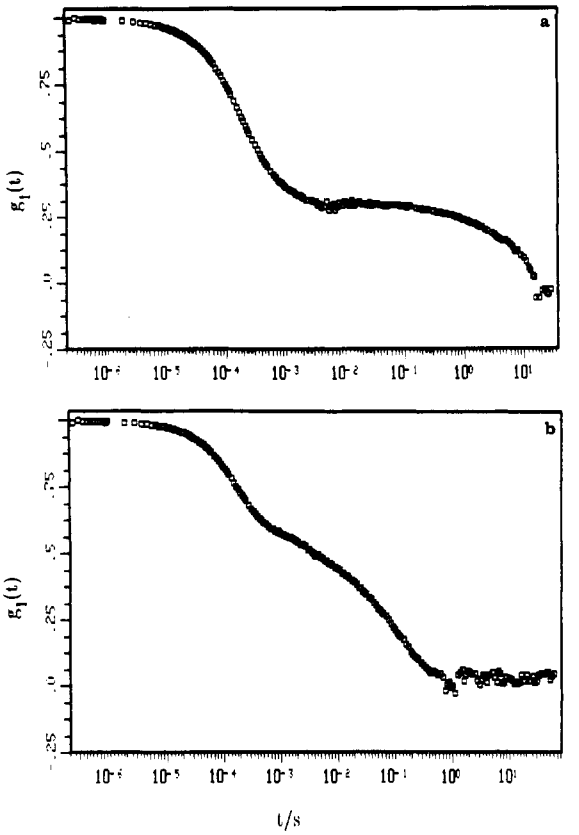

Figure 13. Time correlation function of $PMC_{11}E_8$-2 in water at c = 240 g/L and T = 52 °C (a) and T = 20 °C (b).

Table VI
Results from CONTIN Analysis of the Time Correlation Function of $PMC_{11}E_8$-2 in Water at 52 °C: Concentration Dependence

c, g/cm³	D_{coop}, cm²/s	D_{slow}, cm²/s	c, g/cm³	D_{coop}, cm²/s	D_{slow}, cm²/s
111	4.9×10^{-7}	2.5×10^{-9}	240	7.4×10^{-7}	7.0×10^{-12}
132	5.1×10^{-7}	1.5×10^{-9}	300	1.3×10^{-6}	1.2×10^{-11}
148	6.0×10^{-7}	9.0×10^{-10}			

Table VII
Results from CONTIN Analysis of the Time Correlation Function of $PMC_{11}E_8$-2 in Water: Temperature Dependence

	c = 240 g/L		c = 300 g/L	
T, °C	D_{coop}, cm²/s	D_{slow}, cm²/s	D_{coop}, cm²/s	D_{slow}, cm²/s
20	7.6×10^{-7}	5×10^{-10}	1×10^{-6}	2.4×10^{-10}
40	7.5×10^{-7}	2×10^{-11}	1.1×10^{-6}	2.4×10^{-11}
52	7.4×10^{-7}	7×10^{-12}	1.3×10^{-6}	1.2×10^{-11}

Dilute Solutions. With the sample of *higher molar mass*, $PMC_{11}E_8$-1, aggregates of about two chains were formed at rather low concentrations. Above this concentration the particle's mass stayed stable, and the solution properties became mainly determined by excluded-volume effects between these particles. Such behavior is typical of a closed aggregation, in which molecules aggregate at a certain concentration. An example for such a process is the formation of micelles. The aggregates are stable against changes in temperature and concentration. In the case of $PMC_{11}E_8$-1, they behave like flexible chains; no indications for a pronounced chain stiffness were observed.

The properties of the single macromolecules were similar to those observed in methanol. The molar mass was slightly higher, which can be caused by an association of small molecules on longer chains due to hydrophobic interaction. The hydrodynamic volume of $PMC_{11}E_8$-1 was by a factor 120 larger than that of the monomer micelle.

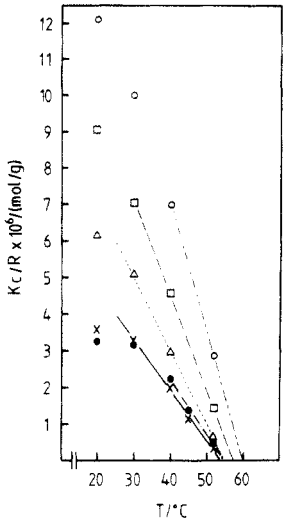

Figure 14. Temperature dependence of the inverse scattering intensity of $PMC_{11}E_8$-2 in water at different concentrations: 2 g/L (○), 10 g/L (×), 33 g/L (△), 52 g/L (□), 73 g/L (●).

The mass, however, was only 15 times larger; thus, the macromolecule was less densely packed than the corresponding monomer micelle.

Extrapolation of measurements above 2 g/L yields the unexpected result that at all temperatures the same M_w is found, which is about 2 times larger than that of the single chain in methanol. A temperature dependence is observed only with A_2. The aggregate's density is the same as that for the single chain.

The *low molar mass* sample, $PMC_{11}E_8$-2, showed no aggregation, as can be seen from the apparent radius of gyration which was independent of concentration at $T \leq 40$ °C (Figure 10), but behavior of a polymer in a poor solvent was found. The scattering intensity increased with temperature; this was not caused by an increase of mass but by a change of thermodynamic interactions. Light scattering at zero scattering angle is given by the osmotic compressibility ($\partial\pi/\partial c$) which is proportional to $\partial\mu/\partial c$ where μ denotes the chemical potential of the solute. At $\partial\mu/\partial c = 0$ the spinodal is obtained, and the reciprocal scattering intensity vanishes at the spinodal. This relationship is used in the pulse-induced critical scattering method in order to investigate phase separation.[30,31] In Figure 14 the reciprocal scattering intensities are shown as a function of temperature, and extrapolation allows us to estimate the miscibility gap (Figure 15). Good agreement with detection by optical microscopy was found. This behavior illustrates the usual solution properties close to a phase separation of $PMC_{11}E_8$-2. With $PMC_{11}E_8$-1 such an influence is not observed.

At 30 °C the Θ-temperature is reached, the polymer is in the undisturbed dimensions, and the characteristic ratio C_∞ can be determined:[32,33]

$$C_\infty = \langle r^2 \rangle / nl^2 \tag{6}$$

with $\langle r^2 \rangle = 6\langle s^2 \rangle$, the mean-square end-to-end distance. l is the length of a C–C bond, and n is number of C–C bonds in the polymer backbone. Assuming a Schulz–Flory molar mass distribution, the square weight-average radius of gyration $\langle s^2 \rangle_w$ can be calculated from the experimentally obtained z-average, and $\langle r^2 \rangle_w = 1300$ nm^2 is obtained. The nl^2 term can be calculated from $l = 0.154$ nm and $n = 2M_w/M_0$, and a characteristic ratio of $C_\infty = 54.2$ is determined. The Kuhn segment length l_k is given by

$$l_k = C_\infty l \tag{7}$$

and $l_k = 8.3$ nm is obtained. The characteristic ratio is much higher than that of poly(methyl methacrylate) ($C_\infty = 8$) and poly(hexadecyl methacrylate) ($C_\infty = 25$).[34] The high value can be the consequence of a strong hydration of the ethylene glycol groups which allows the appearance of side chains more bulky than a pure alkyl chain. However, a high polydispersity can also cause a high C_∞ value. Since the number of Kuhn segments of $PMC_{11}E_8$-2 with 18 is already rather high, the polymer behaves like a flexible chain in solution.

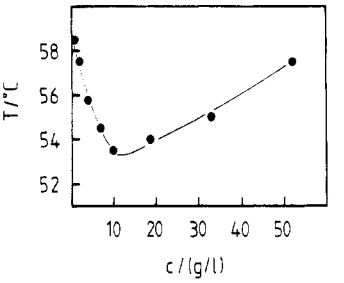

Figure 15. Lower consolute boundary of $PMC_{11}E_8$-2 in water.

The intrinsic viscosity of $PMC_{11}E_8$-2 of $[\eta] = 10$ mL/g is relatively small. $[\eta]$ can be calculated from the Fox–Flory theory of *nondraining* coils:[35]

$$[\eta] = \phi 6^{1.5} \langle s^2 \rangle^{1.5} / M \tag{8}$$

ϕ depends to some extent on the solvent quality, but in the present example the second virial coefficient is with $A_2 = 1 \times 10^{-5}$ mol·cm^3/g^2, already very small, and according to Krigbaum and Carpenter, one has $\phi = 2.5 \times 10^{23}$ mol^{-1}.[36] If again a Schulz–Flory molar mass distribution is assumed, the intrinsic viscosity is calculated to be $[\eta]_{th} = 38$ mL/g, which is about 4 times higher than the experimental value. The coil has to be *partly drained*. The draining parameter h is given as $h = Y/\sqrt{2}$, and the value can be found from experiment and the Kurata–Yamakawa theory[37]

$$\phi(Y) = \frac{M_w(1.5^{3/2})}{\langle s^2 \rangle_z^{3/2}(6^{3/2})}[\eta]_{exp} = 6.55 \times 10^{22} \text{ mol}^{-1} \tag{9}$$

while in the KY theory

$$\phi(Y) = (\pi/6)^{3/2} N_L [YF(Y)] \tag{10}$$

A value of $[YF(Y)] = 0.287$ is found for the Kirkwood–Riseman function.[38] $Y = 0.56$ is then obtained from a plot of $YF(Y)$ as a function of Y that is given by the KY theory, resulting in a draining parameter $h = 0.39$. A second possibility to calculate h makes use of dynamic light scattering data alone. h may be interpreted as the ratio of the nondraining and the draining contribution to the diffusion coefficient. The contribution of the nondraining molecule can be calculated from the radius of gyration. For ideal nondraining coils one finds experimentally[39]

$$\rho = \langle s^2 \rangle_z^{0.5} \langle 1/R_h \rangle_z = 1.27 \tag{11}$$

which together with the radius of gyration yields a hypothetical hydrodynamic radius of $R_h = 14.25$ nm. This corresponds to a diffusion coefficient $D_{ND} = 1.50 \times 10^{-7}$ cm/s^2 for the nondraining limit. Since the experimental diffusion coefficient $D_{z,exp}$ may be expressed as the sum of draining and nondraining contributions, we can write

$$h = (D_{z,exp} - D_{ND})/D_{z,exp} \tag{12}$$

This gives a value of $h = 0.31$ in good agreement with the value derived from intrinsic viscosity data.

The determination of the characteristic ratio and the draining parameter depends on the molar mass distribu-

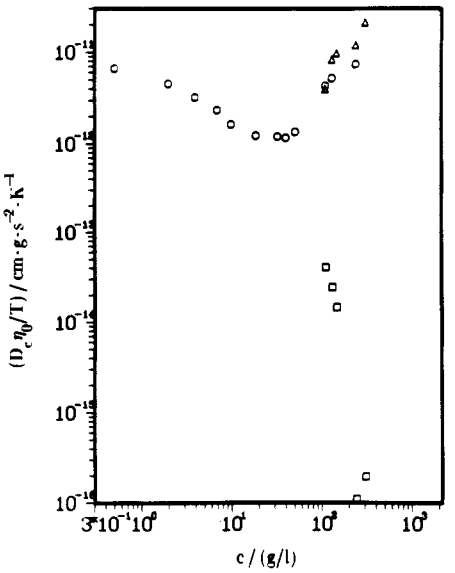

Figure 16. Concentration dependence of the diffusion coefficient of $PMC_{11}E_8$-2 in water at 52 °C: cumulant fits (○); CONTIN, D_{coop} (△) and D_{slow} (□).

tion which could not be determined in aqueous solution. In methanol a polydispersity of $M_w/M_n = 2.9$ was found, and therefore the assumption of a Schulz–Flory distribution may underestimate the polydispersity in water.

Semidilute Solutions. A different behavior of the two samples is also found in semidilute solution. The concentration dependence of the osmotic modulus of $PMC_{11}E_8$-1 followed the behavior of linear flexible chains, whereas a scaling exponent of 2.1 was found with $PMC_{11}E_8$-2 which agrees with the predicted scaling exponent of polymers in Θ-solvents.[22]

An unusual temperature dependence is observed at high concentrations. In static light scattering an increase of the scattering intensity is observed at low angles. Such behavior is known for many semidilute polymer solutions in water and organic solvents and can be explained by the formation of large clusters (or, in other words, long-range heterogeneities[40]). As temperature is increased, excess scattering becomes less pronounced and finally disappears. This observation suggests that the clusters become smaller: they seem to "melt" on heating. In dynamic light scattering, however, a different behavior is found (Figure 13). In many polymer systems the excess scattering is combined with a slow mode in the time correlation function, which can be interpreted as diffusion of the large clusters. This model is supported by the observation that both effects disappear with increasing temperature. For the present polysurfactants this behavior is not found in aqueous solution. While static light scattering displays a common temperature dependence (see Figure 12), in dynamic light scattering unusual effects are observed. This needs a detailed consideration.

For a bimodal system the time correlation function $g_1(t)$ is given by[23]

$$g_1(t) = a_1(q)e^{-D_1q^2t} + a_2(q)e^{-D_2q^2t} \quad (13)$$

with $a_j(q)$ being the amplitude factors which are related to the osmotic compressibilities of the two components. Thus, the height of the plateau in Figure 13 is correlated with the osmotic compressibility of the clusters, and the same temperature dependence was found as in static light scattering. The plateau value was smaller at 52 °C than at lower temperatures, but the slow relaxation time itself increased, and the fast relaxation time remained stable. Results from CONTIN analysis are summarized in Tables VI and VII. The concentration dependence of the two modes at 52 °C is shown in Figure 16, and power law exponents of +0.88 and −6.3 were found for D_{coop} and D_{slow}, respectively. The observation of a slow mode in dynamic light scattering and an unperturbed static light scattering curve means that the prefactors a_1 and a_2 in eq 13 have a similar angular dependence. In other words, the slow mode is not caused by long-range heterogeneities. An increase in friction, which does not enter the static light scattering experiment, can be a reason for the slow mode and is discussed now. An increase of η with increasing temperature was observed in viscosity measurements. Besides, it is known from a study of the $C_{14}E_8$ surfactant that micelles aggregate at higher temperatures.[13] As driving force a loss of bound water is discussed, leading to stronger interaction between ethylene glycol groups, although it has to be noticed that even close to the phase separation micelles are still strongly hydrated.[42] Nevertheless, even a little dehydration can cause strong interaction between ethylene glycol groups and by that coupling the dynamics of many chains. The formation of such a physical network could explain that the static heterogeneities become smaller and the dynamics become slower with increasing temperature.

Recently, Eisele et al. reported on a study of aqueous solutions of poly(vinylcaprolactam).[43] In this case small-angle excess scattering and slow mode disappeared upon heating and it was concluded that hydrophobic interaction was not responsible for the cluster formation. The case of polysurfactant, however, is more complex, since both hydrophobic interactions and hydrogen bonds are present.

6. Conclusions

This study on the solution properties of nonionic polysurfactants reveals uncommon behavior. The polymer properties could be investigated in methanol as the nonaqueous solvent. Both samples behaved like common linear flexible macromolecules in dilute and semidilute solution. At high concentrations a slow mode of motion was detected in the time correlation function, indicating the formation of clusters, which became smaller when the temperature was increased.

Separation between polymer and surfactant properties in aqueous solution was more difficult. A strong influence of the chain length was observed, and both samples revealed different behavior as the monomer micelle. The longer chain, $PMC_{11}E_8$-1, formed aggregates of doubled molar mass at concentrations above 2 g/L. These aggregates do not change their structure with temperature and concentration, which is typical of a closed aggregation. The ρ-parameter and the concentration dependence of the osmotic modulus showed typical flexible-chain behavior. No indications for a pronounced stiffening of the backbone or rodlike structures were found. The shorter chain $PMC_{11}E_8$-2 obeyed different properties. No association but a strong influence of temperature was observed which can be explained by a decrease of the solvent's quality with increasing temperature.

In semidilute solution cluster formation was observed, which showed an unusual temperature dependence. The small-angle excess scattering decreased upon heating, whereas the relaxation time of the slow mode became even longer. This effect can be explained by a hydrodynamic coupling between different chains due to hydrophobic interaction. These lyotropic liquid crystalline polymers therefore revealed different behavior compared to thermotropic liquid crystalline polymers. In semidilute solution of thermotropic liquid crystalline polymers the

cluster formation was independent of chain length but governed by the segment concentration.[25,44]

The different behavior of monomeric and polymeric surfactants in aqueous solution demonstrates the strong correlation between molar mass and solution structure. Amphiphilic molecules try to minimize the contact area of hydrophobic groups with water molecules. With monomeric surfactants the aggregation number of micelles is determined by equilibrium thermodynamics. In polymeric surfactants, however, topological constraints are imposed to the system. If the degree of polymerization exceeds the aggregation number of the monomer micelle, nonsaturated sites of the molecules become available and *inter*molecular interactions occur. In the case of $PMC_{11}E_8$-1 typical surfactant behavior was found: the unfavorable interactions lead to the formation of aggregates which now allow internal stabilization, and common excluded-volume repulsion among aggregates is observed at higher concentrations. With $PMC_{11}E_8$-2, on the other hand, such a stabilization seems not to be possible and a strong influence of the miscibility gap is observed. This feature is very surprising because the molecular weights differ only by a factor of 2. A difference in the change of entropy connected with the aggregation of two or four molecules may be one reason for the different behavior of the two samples. A second reason could be a different tacticity. Both sample were radically polymerized, but different solvents were used that might result in a different tacticity.

Since the thermodynamics can be easily changed by varying the degree of polymerization, these systems are suited for further theoretical studies and industrial applications.

Acknowledgment. We cordially thank the Deutsche Forschungsgemeinschaft for financial support within the Sonderforschungsbereich 60. W.R. thanks the Graduiertenkolleg Polymerwissenschaften for a scholarship.

References and Notes

(1) Degiorgio, V. In *Physics of Amphiphiles: Micelles, Vesicles and Microemulsions*; Degiorgio, V., Corti, M., Eds.; North-Holland: Amsterdam, The Netherlands, 1985.
(2) *Surfactants in Solution*; Mittal, K. L., Bothorel, P., Eds.; Plenum Press: New York, 1986; Vols. 4–6.
(3) Surfactant Science Series Vol. 23; Schick, M. J., Ed.; Dekker: New York, 1987.
(4) Tiddy, G. J. T. *Phys. Rep.* **1980**, *57*, 1.
(5) Tanford, C. *The Hydrophobic Effect*; Wiley: New York, 1973.
(6) Frank, H. S. In *Water: A Comprehensive Treatise*; Frank, F., Ed.; Plenum Press: New York, 1972; Vol. 1.
(7) Frank, F. In *Water: A Comprehensive Treatise*; Frank, F., Ed.; Plenum Press: New York, 1975; Vol. 4.
(8) Ravey, J. C. *J. Colloid Interface Sci.* **1983**, *94*, 289.
(9) Cebula, D. J.; Ottewill, R. H. *Colloid Polym. Sci.* **1982**, *260*, 1182.
(10) Brown, W.; Johnsen, R.; Stilbs, P.; Lindman, B. *J. Phys. Chem.* **1983**, *87*, 4548.
(11) Zulauf, M.; Rosenbusch, J. P. *J. Phys. Chem.* **1983**, *87*, 856.
(12) Zulauf, M.; Weckström, K.; Hayter, J. B.; Degirogio, V.; Corti, M. *J. Phys. Chem.* **1985**, *89*, 3411.
(13) Richtering, W. H.; Burchard, W.; Jahns, E.; Finkelmann, H. *J. Phys. Chem.* **1988**, *92*, 6032.
(14) Kelker, H.; Hatz, R. *Handbook of Liquid Crystals*; Verlag Chemie: Weinheim, Germany, 1980.
(15) Löffler, R.; Richtering, H. W.; Finkelmann, H.; Burchard, W. *J. Phys. Chem.*, in press.
(16) Löffler, R. Ph.D. Thesis, Albert-Ludwigs-Universität Freiburg, Freiburg, Germany, 1990. Löffler, R.; Finkelmann, H. Manuscript in preparation.
(17) *Light Scattering from Polymer Solutions*; Huglin, M. B., Ed. Academic: London, 1972.
(18) Ohta, T.; Oono, Y. *Phys. Lett. A* **1982**, *89A*, 460.
(19) Freed, K. *Renormalization Group Theory of Macromolecules*; Wiley: New York, 1987.
(20) Carnahan, N. F.; Starling, K. E. *J. Chem. Phys.* **1969**, *51*, 635.
(21) Burchard, W. *Makromol. Chem., Macromol. Symp.* **1988**, *18*, 1.
(22) de Gennes, P.-G. *Scaling Concepts in Polymer Physics*; Cornell University Press: Ithaca, NY, 1979.
(23) Berne, B. J.; Pecora, R. *Dynamic Light Scattering*; Wiley: New York, 1976.
(24) Yamakawa, H. *Modern Theory of Polymer Solutions*; Harper & Row: New York, 1971.
(25) Richtering, W. Ph.D. Thesis, Albert-Ludwigs-Universität Freiburg, Freiburg, Germany, 1990.
(26) Provencher, S. W. *Comput. Phys. Commun.* **1982**, *27*, 213.
(27) Burchard, W.; Schmidt, M.; Stockmayer, W. H. *Macromolecules* **1980**, *13*, 580.
(28) Eisele, M.; Burchard, W. *Macromolecules* **1984**, *17*, 1636.
(29) Elias, H. G. *Makromoleküle*; Hüthig & Wepf: Basel, Switzerland, 1981.
(30) Gordon, M.; Kajiwara, K. *Plaste Kautsch.* **1972**, *4*, 245.
(31) Gordon, M.; Kajiwara, K.; Charlesby, A. *Eur. Polym. J.* **1974**, *11*, 385.
(32) Flory, P. J. *Principles of Polymer Chemistry*; Cornell University Press: Ithaca, NY, 1953.
(33) Flory, P. J. *Statistical Mechanics of Chain Molecules*; Interscience: New York, 1969.
(34) Brandrup, J.; Immergut, E. H. *Polymer Handbook*; Wiley: New York, 1975.
(35) Fox, T. J.; Flory, P. J. *J. Am. Chem. Soc.* **1951**, *73*, 1904.
(36) Krigbaum, W. R.; Carpenter, D. K. *J. Phys. Chem.* **1955**, *59*, 1166.
(37) Kurata, M.; Yamakawa, H. *J. Chem. Phys.* **1958**, *29*, 311.
(38) Kirkwood, J. G.; Riseman, J. *J. Chem. Phys.* **1948**, *16*, 656.
(39) Schmidt, M.; Burchard, W. *Macromolecules* **1981**, *14*, 210.
(40) Koberstein, J. T.; Picot, C.; Benoit, H. *Polymer* **1985**, *28*, 673.
(41) Brown, W.; Stepanek, P. *Macromolecules* **1988**, *21*, 1791.
(42) Nilsson, P. G.; Lindman, B. *J. Phys. Chem.* **1983**, *87*, 4756.
(43) Eisele, M. Ph.D. Thesis, Albert-Ludwigs-Universität Freiburg, Freiburg, Germany, 1988.
(44) Richtering, W.; Gleim, W.; Burchard, W. *Macromolecules*, accepted.

Registry No. $H_2C{=}C(CH_3)C(O)O(CH_2)_{11}(OCH_2CH_2)_8OMe$, 129522-76-5; $H_2C{=}C(CH_3)C(O)O(CH_2)_{11}(OCH_2CH_2)_8OMe$ (homopolymer), 141397-81-1; CH_3OH, 67-56-1.